Published in final edited form as:
Biochim Biophys Acta. 2007 September ; 1768(9): 2182–2194. doi:10.1016/j.bbamem.2007.05.012.

Fluorescence probe partitioning between L_o/L_d phases in lipid membranes

Tobias Baumgart[1], **Geoff Hunt**[2], **Elaine R. Farkas**[1], **Watt W. Webb**[1,*], and **Gerald W. Feigenson**[2]

1 *School of Applied and Engineering Physics, Cornell University, Ithaca, NY, 14853*

2 *Department of Molecular Biology and Genetics, Cornell University, Ithaca, NY, 14853*

Summary

Fluorescence microscopy imaging is an important technique for studying lipid membranes and is increasingly being used for examining lipid bilayer membranes, especially those showing macroscopic coexisting domains. Lipid phase coexistence is a phenomenon of potential biological significance. The identification of lipid membrane heterogeneity by fluorescence microscopy relies on membrane markers with well-defined partitioning behavior. While the partitioning of fluorophores between gel and liquid-disordered phases has been extensively characterized, the same is not true for coexisting liquid phases.

We have used fluorescence microscopy imaging to examine a large variety of lipid membrane markers for their liquid phase partitioning in membranes with various lipid compositions. Most fluorescent lipid analogs are found to partition strongly into the liquid-disordered (L_d) phase. In contrast, some fluorescent polycyclic aromatic hydrocarbons with a flat ring system were found to partition equally, but others partition preferentially into liquid-ordered (L_o) phases. We have found these fluorescent markers effective for identification of coexisting macroscopic membrane phases in ternary lipid systems composed of phospholipids and cholesterol.

Keywords

liquid ordered; liquid disordered; fluorescence microscopy; probe partitioning; liposome; vesicle

Introduction

The “raft hypothesis,” which proposes that biological membranes laterally segregate into biologically relevant entities based on lipid phase separations, is currently a matter of considerable controversy and has been the focus of numerous reviews [1–13]. Despite enormous efforts to understand lateral membrane heterogeneities, the membrane phase behavior of live cells, and even simple model membrane mixtures, is currently far from being understood. For example, complex experiments that cause drastic reorganization of biological membranes, e.g. detergent resistance or major changes in cholesterol concentration, have been used to infer molecular-level details of membrane structure, leaving considerable uncertainty

*Corresponding Author: Watt W. Webb, 212 Clark Hall, Cornell University, Ithaca, NY, 14853-2501, Phone: (607) 255-3331, Fax: (607) 255-7658, email E-mail: www2@cornell.edu.

regarding the partitioning of membrane associated components. A variety of fluorescence approaches have been used to examine the existence and nature of lipid heterogeneities in relatively unperturbed biological membranes, including imaging of plasma membrane lipid heterogeneities [14,15], fluorescence polarization studies [16], fluorescence red shift imaging [17], fluorescence resonance energy transfer imaging [18], and single particle tracking [19]. For the fluorescent probes used in these and other studies, the partition coefficients of fluorophores between liquid-ordered (L_o, the putative "raft" phase) and liquid-disordered (L_o or L_d) phases are unknown. Lipid model membranes provide a means to examine the partitioning behavior of membrane fluorophores between membrane phases, for defined and equilibrated membrane compositions. The partitioning of fluorescence probes between membrane phases has been examined by a variety of techniques [20,21], and a wide range of fluorescent probes has been employed to study membrane heterogeneity [20,22].

Optically resolvable liquid-disordered / liquid-ordered phase domains in lipid model membranes have been studied by fluorescence microscopy in lipid bilayer membranes from mixtures involving at least three components [23–28]. These studies were preceded by fluorescence microscopy studies of gel / L_d phase coexistence in lipid bilayers [29–32].

Most studies to date have examined the partitioning of fluorophores between gel and L_d phase [33–39]. An important finding from this body of research is that gel partitioning is increased for fluorophores with saturated chains that approximately match the thickness of one leaflet of the gel host membrane [33,35]. Probe moieties linked to alkyl chains at the chain end versus positions closer to the headgroup of amphiphilic membrane components showed larger preference for gel phases [34,36], probably due to decreased perturbation of the packing of the gel. Fluorescent lipid probes with unsaturated chains are found to partition into the disordered liquid phase [38].

Due to the need to interpret studies from fluorescence microscopy and to elucidate the biological relevance of phase coexistence, the partitioning of fluorophores between L_o/L_d phases is increasingly being addressed [40–44]. Importantly, short chain sphingolipid probes were found to have relatively low partitioning into membrane phases with putative raft-like compositions [40]. Furthermore, increased partitioning into the L_d phase versus the L_o phase was found for increasing degree of unsaturation and decreasing chain lengths, as in the case of bimane-labeled diacyl phospholipid probes [41], similar to the findings for gel/L_d coexistence mentioned above. Corresponding findings were reported in [38].

The present study examines the partitioning of fluorophores, many of which might be used for imaging lipid bilayer membranes with fluorescence microscopy techniques. To facilitate systematic comparisons, a large number of fluorophores are examined by a fixed protocol.

We first discuss the partitioning of *lipid* fluorophores between coexisting L_o and L_d phases for two different ternary lipid mixtures. These labeled lipids have a fluorophore either at the head group or attached to the hydrocarbon chain, or are fluorescent cholesterol derivatives or analogs. Fluorophore partitioning is determined by qualitatively comparing fluorescence intensities in coexisting domains. We discuss experimental limitations in deducing fluorophore partitioning from fluorescence microscopy imaging. We then elucidate the partitioning of several fluorescent polycyclic aromatic hydrocarbons (PAHs), because the PAH perylene was recently found to allow imaging of liquid-ordered domains coexisting with L_d domains [28]. Our findings indicate that PAHs, in contrast to the majority of fluorescent membrane markers, show a weak to pronounced affinity for L_o versus L_d phases. Finally, we determine the orientational ordering of PAHs in differing membrane phases by polarized fluorescence microscopy.

Materials and Methods

Phospholipids and cholesterol

Brain sphingomyelin (SPM), dioleoylphosphatidylcholine (DOPC), dioleoylphosphatidylglycerol (DOPG), distearoylphosphatidylcholine (DSPC) and N-caproylamine dipalmitoylphosphatidylethanolamine were purchased from Avanti Polar Lipids, Inc. (Alabaster, AL) and used without purification after phospholipid purity was confirmed by thin-layer chromatography. Phospholipid stock solutions were quantitated by means of a phosphate assay [31]. Cholesterol (chol) was obtained from Nu Chek Prep (Elysian, MN) or Avanti Polar Lipids, and a stock solution was prepared in chloroform by standard quantitative techniques.

Fluorescent probes

The fluorescent probes N-(Lissamine Rhodamine B sulfonyl) dioleoyl phosphatidylethanolamine (Liss-Rho-DOPE), 1,2-dipalmitoyl-sn-glycero-3-phosphoethanolamine-N-(Lissamine Rhodamine B Sulfonyl) (Liss-Rho-DPPE), N-(7-nitro-2-1,3-benzoxadiazol-4-yl) dipalmitoyl phosphatidylethanolamine (NBD-DPPE), 1,2-dipalmitoyl-*sn*-glycero-3-phosphoethanolamine-N-(1-Texas Red hexanoyl), and 1,2-dioleoyl-sn-glycero-3-phosphoethanolamine (7-nitro-2-1,3-benzoxadiazol-4-yl) (NBD-DOPE), were purchased from Avanti Polar Lipids, Inc (Alabaster, AL).

The fluorescent probes N-(4,4-difluoro-5,7-dimethyl-4-bora-3a,4a-diaza-s-indacene-3-dodecanoyl)sphingosyl phosphocholine (Bodipy-C_{12}-SPM), N-(4,4-difluoro-5,7-dimethyl-4-bora-3a,4a-diaza-s-indacene-3-pentanoyl)sphingosyl phosphocholine (Bodipy-C_5-SPM), 2-(4,4-difluoro-5,7-dimethyl-4-bora-3a,4a-diaza-s-indacene-3-pentanoyl)-1-hexadecanoyl-sn-glycero-2-phosphocholine (Bodipy-PC), 3,3′-dilinoleyloxacarbocyanine perchlorate (DiO-C18:2), 1,1′-didodecyl-3,3,3′,3′-tetramethylindocarbocyanine perchlorate (DiI-C12:0), 1,1′-dihexadecyl-3,3,3′,3′-tetramethylindocarbocyanine perchlorate (DiI-C16:0), 1,1′-dioctadecyl-3,3,3′,3′-tetramethylindocarbocyanine perchlorate (DiI-C18:0), 1,1′-dieicosanyl-3,3,3′,3′-tetramethylindocarbocyanine perchlorate (DiI-C20:0), 1,1′-didocosanyl-3,3,3′,3′-tetramethylindocarbocyanine perchlorate (DiI-C22:0), 1,1′-dioleoyl-3,3,3′,3′-tetramethylindocarbocyanine perchlorate (DiI-C18:1), 3,6-bis (diethylamino)-9-(2-octadecyloxy) carbonyl)phenyl, chloride (R18), and 22-(*N*-(7-nitrobenz-2-oxa-1,3- diazol-4-yl)amino)-23,24-bisnor-5- cholen-3-ol (NBD-chol) were purchased from Molecular Probes (Eugene, OR).

The fluorophore Texas-red N-caproylamine DPPE was synthesized from N-caproyl dipalmitoylphosphatidylethanolamine according to a procedure described in [45]. Cholestatrienol was synthesized according to Fischer et al. [46].

Naphtho-[2,3a-]pyrene, perylene, and rubicene, and N,N, bis-dimethylphenyl 2,4,6,8, perylenetetracarbonyl diamide (PERY) were purchased from Sigma-Aldrich Corp. (St. Louis, MO). Terrylene was obtained from Chiron AS Chemicals (Trondheim, Norway).

Preparing GUVs

Giant unilamellar vesicles (GUVs) were prepared according to the procedure described by Akashi et al. [47], with a few variations. Alternatively, the method of electroswelling was employed [48]. Both methods led to identical phase behavior and equivalent probe partitioning, determined by fluorescence microscopy, excluding electrode effects [49] to contribute to our findings. In both cases, GUVs were formed at a temperature of 65°C, which ensured vesicle formation from homogenous bilayer membranes. In the case of the Akashi method, the buffer was 2 mM Pipes, 10 mM KCl, and 1 mM EDTA, pH = 7.0. Stock solutions of DOPC in

chloroform contained 10 mol% DOPG, since charged phospholipids are necessary for preparing GUVs by this method [47]. Stock solutions of SPM and DSPC in chloroform contained no additional charged lipids. With the electroswelling method, stock solutions did not contain charged lipids. For this method, GUVs were swelled using an alternating electric field applied for 2h in a sucrose solution (100mM) [48]. Following either preparation method, GUVs were slowly cooled (~1–2°C/h) to room temperature (~23°C), deposited onto #1 coverslips, and enclosed by a clean glass slide containing a ring of silicone high-vacuum grease as a surrounding seal and spacer.

Ternary lipid mixtures used to prepare GUVs were SPM/DOPC/chol and DSPC/DOPC/chol. The vesicle composition for vesicles with liquid phase coexistence was 27/50/23 (molar ratios of SPM or DSPC/DOPC/chol), except for the vesicle shown in Figure 3e and 3f, which had a composition of SPM/DOPC/chol = 30/45/25. Most fluorescent probes were added at a concentration of 0.1 mol%. The fluorescent probes Bodipy-C_{12}-SPM, Bodipy-C_5-SPM, and NBD-chol were added at concentrations of 0.2 mol%. The fluorescent probes perylene, naphthopyrene, rubicene and terrylene were added at concentrations of 0.5 mol%.

Microscopy

GUVs were imaged with either confocal microscopy using a Leica TCS SP2 spectral confocal system (Leica Microsystems Inc, Bannockburn, IL) or by two-photon excitation microscopy using a homebuilt multiphoton laser scanning microscope (W.R. Zipfel, Cornell University) based on a Bio-Rad 1024 scanhead (Bio-Rad, Richmond, CA), using a two-photon excitation wavelength of $\lambda = 750$ nm. In case of confocal one-photon excitation microscopy, the following wavelengths were used for excitation: 458 nm (naphthopyrene), 488 nm (Bodipy, DiO, NBD, rubicene, PERY), and 568 nm (DiI, Lissamine rhodamine, Texas red, R18). Cholestatrienol was imaged by wide-field illumination using a bandpass excitation filter centered at 340 nm (width 30 nm). For all probes examined, partitioning was determined for vesicles labeled with one dye only to avoid bleed-through into different detector channels. Membrane phase assignment was checked by double labeling vesicles with the probe of interest and another probe of known partitioning behavior. Angular emission patterns were determined by imaging equatorial sections of homogenous vesicles using linearly polarized light, and extracting the angular intensity profiles from the obtained fluorescence micrographs by means of a tracing algorithm. Each angular profile consisted of averaged measurements of ten different vesicles. All images were obtained at room temperature.

Results

A total of 26 lipid membrane probes (see Figure 1 and 2 for molecular structures) were used to examine the principles that govern the partitioning of membrane fluorophores between coexisting liquid membrane phases in giant unilamellar vesicles. In order to identify molecular factors governing probe partitioning, we examined dye distributions between two coexisting liquid phases, a liquid ordered (L_o) and a liquid disordered (L_d) phase, in vesicles made of ternary lipid mixtures with identical compositions. In order to determine potential differences in probe partitioning in vesicles with the same lipid ratios but different ordered phase-preferring lipid type, we compared fluorophore partitioning in two different lipid systems. The ternary lipid mixtures used were SPM/DOPC/cholesterol and DSPC/DOPC/cholesterol. All vesicles (except where indicated) had a composition of 27/50/23 (molar ratios of SPM or DSPC/DOPC/cholesterol).

Phase assignment of GUVs imaged by fluorescence microscopy was accomplished by determining the following membrane phase features: a) area fraction, b) continuity (connectivity), and c) partitioning of fluorophores with known partitioning behavior. According to published phase diagrams of ternary lipid mixtures [26,32], the composition of

our vesicles leads to segregation into a DOPC rich majority L_d phase, and a DSPC- or SPM-rich L_o minority phase. Phase assignment was verified using the fluorophore Liss-Rho-DOPE, which had previously been found to partition strongly out of L_o phases coexisting with L_d phases [23].

Figures 1 and 2 show the molecular structures of all the fluorophores that were examined. The dyes may be categorized as follows: a) phospholipids with unsaturated acyl chains and a headgroup label (NBD-DOPE and Liss-Rho-DOPE); b) phospholipids with saturated acyl chains and a headgroup label (NBD-DPPE, Texas-Red-DPPE and Liss-Rho-DPPE); c) phospholipids with saturated acyl chains and a label attached to the headgroup via a caproyl spacer (Texas-red-N-caproylamine-DPPE); d) carbocyanine dyes with saturated hydrocarbon chains (DiI C_n:0 with n = 12, 16, 18, 20, 22); e) carbocyanine dyes with unsaturated lipid chains (DiO C18:2 (fast) and DiI C18:1); f) chain-labeled phospholipids (Bodipy-C5-PC, Bodipy-C5-SPM, and Bodipy-C12-SPM, Bodipy-ceramide); g) single alkyl chain membrane probes (R18); h) a labeled cholesterol analog (NBD-chol); i) the fluorescent cholesterol analog cholestatrienol; j) fluorescent polycyclic aromatic hydrocarbons (naphthopyrene, rubicene, perylene, terrylene, and “PERY”); k) the fluorescent hydrophobic membrane marker DPH.

Table 1 and Table 2 summarize the partitioning behavior of all the fluorescent membrane probes used in this study. In these tables, the partitioning of fluorophores is divided into three categories distinguishing L_o phase or L_d phase preference, and equal partitioning into either L_o or L_d phases. In principle, fluorescence microscopy allows the quantitation of fluorophore partitioning (in terms of *partition coefficients*). Such a quantitative approach is challenging beyond the usual problems of background subtraction and shading corrections over the image, requiring careful correction for effects such as concentration-dependent self-quenching, the influence of each membrane phase on fluorescence intensity due to fluorophore environmental sensitivity, and selective excitation due to confined fluorophore orientations in differing phases (see below). Therefore, we report here the qualitative partitioning behavior of these 26 probes.

Table 1 summarizes the observed partitioning behavior of all fluorophores in the SPM system. Qualitatively similar partitioning behavior was found in the DSPC system, with the important exception of saturated chain DiI dyes (see below). The behavior of these dyes is depicted in Table 2.

In every case, fluorescent membrane markers that contained unsaturated alkyl chains or fluorophore-labeled chains as membrane anchors were observed by confocal fluorescence microscopy to partition strongly out of the L_o phase, and into the L_d phase. This overarching observation applies to both the DSPC and the SPM ternary lipid systems. A representative example is shown in Figure 3a, which displays a hemispherical projection of a vesicle (DSPC system) labeled with the fluorophore Liss-Rho-DOPE. In this vesicle, a brightly labeled L_d domain is found (in Figure 3a and all following images of phase separated vesicles, a white arrow points to the L_d phase), whereas in the L_o phase matrix, hardly any fluorescence could be detected. Liquid-disordered phases of the mixtures used in the present study are enriched in DOPC relative to the coexisting liquid-ordered phases. Strong partitioning into the L_d phase (coexisting with an L_o phase) of probes with unsaturated alkyl chains is therefore expected and has been observed in previous microscopy studies [23].

Lipids labeled in the chain region with the Bodipy fluorophore partitioned preferentially into the L_d phase for both mixtures examined in this study. The membrane dye Bodipy-PC had previously been observed to partition preferentially into L_d phases coexisting with gel phase domains [30]. Figure 3b shows a vesicle of the DSPC system in which Bodipy-PC shows fluorescence in L_d phase domains rather than in the coexisting L_o phase domains. Note that inhomogeneous fluorescence intensity levels within homogenous membrane phases in Figures

3 and 4 result from vesicle movement during imaging, membrane assemblies near the imaged vesicle, and collection of sub-optimal numbers of confocal slices for hemispherical projections. The sphingomyelin-derived fluorophore Bodipy-C5-SPM has been interpreted in the past to mimic the properties of endogenous sphingomyelin in biological cell membranes, particularly to study intracellular membrane trafficking pathways [50–52]. The partitioning of Bodipy-C5-SPM, Bodipy-C12-SPM and Bodipy-Ceramide were therefore examined in vesicles containing sphingomyelin-enriched L_o domains. All three dyes are observed to partition strongly out of the sphingomyelin-rich L_o phase matrix and into L_d phase domains (images not shown), both in the DSPC and in the SPM system. This finding is in accordance with results from Wang and Silvius, who determined probe partitioning by an inter-vesicle partitioning method [40]. They found Bodipy-C5-SPM to partition preferentially out of sphingomyelin-enriched L_o domains. As these authors noted, caution is needed when relating studies of membrane trafficking with short chain fluorescent sphingomyelin probes to heterogeneous membrane distributions of endogenous sphingomyelins [40].

Since L_o phases are enriched in long-chain saturated lipids, the present study examined the partitioning behavior of long and saturated chain, head group labeled membrane dyes derived from DPPE. Dietrich et al., using planar supported membranes of the SPM/POPC/chol system [24] (composition 0.25/0.5/0.25), observed that the fluorophore NBD-DPPE partitioned with modest preference into the L_o phase, while the fluorophore Texas-red-DPPE strongly preferred the L_d phase [24]. Similar partitioning behavior of Texas-red-DPPE was also found by Veatch et al. [26] in GUVs of a range of different compositions. We found that for all DPPE-derived probes used in the present study (see Table 1), strong preference for liquid-disordered phases was observed in both SPM and DSPC systems. Figures 3c and 3d show this partitioning behavior for the fluorophores NBD-DPPE and Liss-Rho-DPPE, respectively, in the DSPC system. This finding implies that the presence of a bulky fluorophore in the headgroup region disturbs lipid packing in that part of an L_o phase membrane, which leads to preferential exclusion of these fluorophores from the L_o phase if the L_o phase coexists with a disordered liquid phase. This explanation is supported by Samsonov et al., who found the fluorophore N-Bodipy-GM1 to be enriched in L_o phase domains [23]. In that case, the fluorophore was effectively separated from the headgroup region by a sugar spacer. We therefore synthesized N-caproylamine-Texas-Red-DPPE, where the fluorophore is separated from the headgroup region by a 6-carbon caproyl spacer. Again, however, strong partitioning of this dye out of L_o and into coexisting L_d phases was observed in both of the ternary systems examined. This effect is likely not due to exclusion of the ethanolamine part of the headgroup from the PC-rich L_o region, because the Silvius group found that the nature of the lipid headgroup only weakly influenced lipid partitioning between L_o and L_d phases when comparing phosphatidylcholine, sphingomyelin, glycosphingolipids, and the ganglioside GM1 [43]. Thus, despite the presence of a caproyl spacer, the partitioning of the membrane probe N-caproyl-Texas-Red-DPPE is probably dominated by the presence of a large and bulky fluorophore attached to the ethanolamine headgroup. Based on this finding, we suggest that the saccharide moieties of gangliosides must be able to pack more efficiently into the headgroup region of SPM-rich L_o phases or alternatively, more effectively prevent the bulky fluorophore from perturbing the membrane surface.

The dialkylcarbocyanine dyes, DiI, are among the most widely used fluorescent membrane probes, in part because of brightness and photostability, and in part because of their availability with a variety of hydrocarbon chains. These dyes have been employed for imaging membrane heterogeneity in cellular membranes [14,15], and some were found to enrich in ordered regions with properties similar to detergent resistant membranes [15], which have been assumed to be in the L_o phase state [53]. However, as shown in Figures 4a to 4e, none of these DiI probes preferentially partitioned into sphingomyelin-rich L_o domains. DiI dyes with saturated chains of lengths 12, 16, 18, 20 and 22 carbons partitioned strongly out of L_o and into the L_d phase

in the SPM system. However, in the DSPC system, DiI with chain lengths 18, 20 and 22 partitioned preferentially into the L_o phase (see Figure 4i–j), whereas the shorter chain lengths (12 and 16 carbons) partitioned into the L_d phase (see Figure 4g and 4h). The partitioning behavior of DiI dyes in both of the ternary systems is summarized in Table 2. The finding of a difference in long chain DiI dye partitioning in quasi-ternary SPM and DSPC systems is supported by an equivalent previous result for the DiI C18 dye [54].

Indocarbocyanine fluorophores with unsaturated alkyl chains (DiI C18:1, fast DiO) partitioned strongly into the L_d phase in both the SPM and DSPC systems. The single chain amphiphilic fluorophore R18 was also observed to partition strongly out of L_o domains and into L_d domains, for both the DSPC and the SPM systems (images not shown).

Cholesterol is expected to enrich in L_o phases relative to coexisting L_d phases, according to the tie line directions in lipid systems similar to the ones examined in the present research [55]. However, the cholesterol derivative NBD-chol partitioned out of L_o domains and into L_d domains (images not shown). This finding underscores the fact that NBD-chol is a label that does not mimic the properties of unmodified cholesterol, as has been pointed out previously [56]. We found that cholestatrienol does enrich in L_o domains in the sphingomyelin system, as indicated in Fig 3e–f. The fluorophore, however, bleaches quickly and high quality images are difficult to obtain. It has been found that cholestatrienol, a fluorescent cholesterol derivative, mimics endogenous cholesterol even better [56] than the commercially available fluorescent dehydroergosterol that has been employed as a fluorescent cholesterol analog for microscopy studies of cellular membranes [15].

Partitioning of fluorescent polycyclic aromatic hydrocarbons

Several fluorescent polycyclic aromatic hydrocarbons show sufficient quantum yield, photostability and wavelength characteristics to make them suitable for fluorescence microscopy. Their partitioning behavior was therefore of great interest.

In a search for probes that allow imaging L_o phase membranes, we focused on polycyclic aromatic hydrocarbons that were not attached to lipid analogs [44]. We tested the possibility that these dyes would mimic the packing properties of cholesterol, given their flat, disk-shaped molecular structure.

The highly photostable fluorophore perylene has long been used as a fluorescent membrane dye for spectroscopic studies [57–59]. More recently, perylene has enabled two-color fluorescence microscopy of coexisting liquid phases. Perylene was found to preferentially label L_o phases in ternary lipid mixtures containing *egg* sphingomyelin, DOPC, and cholesterol [28]. Figure 5a shows that perylene does not show preferential partitioning in ternary mixtures containing *brain* sphingomyelin, though (compare 5b which shows Liss-Rho-DOPE partitioning in the same vesicle as 5a to indicate phase coexistence). Rubicene is another polycyclic aromatic hydrocarbon with high photostability that can be used for microscopy imaging. Similar to perylene perylene, rubicene showed partitioning that very weakly favors the L_o phase between liquid-ordered and disordered phases (data not shown). Naphthopyrene shows stronger partitioning into L_o phases in the brain sphingomyelin system (Figure 5c, compare 5d which shows Liss-Rho-DOPE partitioning in the same vesicle). Similarly, preferential L_o phase partitioning is found with the fluorophore terrylene (Figure 5e).

In order to further examine the molecular features that lead fluorophores to enrich in the liquid-ordered phase, we labeled vesicles with the bi-substituted perylene derivative PERY. The bis-dimethylphenyl groups of this fluorophore are known to be able to rotate around the C-N bond [60]. This molecular feature, as well as the polar additions to the perylene backbone, differs from the flat and rigid hydrocarbon disks of the other PAHs studied. As indicated in Figure

6a, PERY is indeed observed to partition strongly out of the ordered and into the disordered liquid phase, in both the SPM and DSPC systems. This observation supports our finding that polycyclic aromatic dyes partition into the L_o phase only in the case of hydrophobic molecules with a rigid ring system that does not obstruct lipid chain packing.

We also examined the partitioning of the membrane fluorophore DPH. Lipid-bound analogs of DPH, and DPH itself, have been used in numerous studies to analyze chain ordering in lipid model membranes [61,62] as well as cellular membranes [16]. The partition coefficients between cholesterol- and DPPC-rich liquid-ordered phases and pure DPPC above the main phase transition temperature (liquid-disordered phase) have been described as being close to unity [16,63]. Figure 6c indicates that in the ternary lipid mixture SPM/DOPC/cholesterol, DPH shows a negligible partitioning difference for the mixing ratio examined in the present study. Similar partitioning was found in the DSPC system. While DPH is a nonpolar fluorophore, it lacks the rigid ring structure that leads to preferred liquid-ordered phase partitioning.

Orientation of hydrophobic membrane markers in L_o and L_d phases

In order to elucidate why disk-shaped hydrophobic polycyclic hydrocarbons partition preferentially into liquid-ordered phases, we qualitatively determined probe orientations with respect to the membrane normal direction by using polarized excitation fluorescence microscopy. To this end, optically homogenous vesicles of either L_d phase or L_o phase state were illuminated with linearly polarized light and imaged in the equatorial planes. Figure 7 compares the intensity patterns of Liss-Rho-DOPE (second image in each panel) versus perylene, naphthopyrene and terrylene, respectively, in L_d phase vesicles (pure DOPC, left column) and L_o phase vesicles (SPM/chol = 1/1, right column). The excitation light polarization direction used for all images shown in Figure 7 is indicated by the white arrow in Figure 7a.

For all three PAHs and for Liss-Rho-DOPE, the directions of absorption and emission dipole moments point roughly along the longest axis of the dye molecule. The angular emission patterns of GUVs obtained with linearly polarized excitation can therefore be used to infer average membrane probe orientations [64–66]. A (headgroup-labeled) Liss-Rho lipid analog was previously found to orient, on average, parallel to the membrane, i.e. transition dipole moments of the fluorophore are tangent to the plane of the membrane [66]. Given the excitation light polarization direction (see arrow in Fig 7), this fluorophore is observed to emit at higher intensities towards left and right parts of the vesicles, as expected. This behavior is shown in Figure 7.

All three PAHs showed approximately uniform angular emission patterns for L_d phase vesicles (consisting of DOPC membranes). This finding seems to indicate random orientations of excitation dipole moments of these PAHs in L_d phase membranes. In contrast to this finding, for L_o phase vesicles, we observed for all three PAHs an angular emission pattern that was rotated by 90° compared to the Liss-Rho-DOPE pattern. This indicates that in the L_o phase, PAH excitation dipole moments are oriented preferentially along the membrane normal. This observation is in accordance with PAHs intercalating into liquid-ordered membranes in a way similar to cholesterol, i.e. by association of the flat surface of a disk shaped molecule with the saturated lipid chains in the L_o phase.

Figure 8 depicts angular normalized fluorescence intensity traces, obtained from microscopy images equivalent to those shown in Figure 7. The relative intensity differences comparing intensity maxima and minima of angular emission patterns (Figure 8) are related to the width of a probe's orientational probability distribution [65,67]. Larger PAHs like terrylene might experience a stronger confinement in lipid membranes compared to smaller PAHs like perylene. Figure 8a–8e indicates that perylene shows a shallower angular emission intensity

profile in L_o phase GUVs consisting of SPM/chol =1/1 compared to naphthopyrene and terrylene in vesicles with the same lipid mixtures. This finding parallels the partitioning tendency of the fluorophores between coexisting L_d and L_o phases described above. Increased orientational confinement compared to pure DOPC membranes is also observed in DOPC membranes containing 30 mol% of cholesterol, as Figures 8e–f show. The ordering effect of cholesterol is weaker in DOPC/chol compared to SPM/chol membranes (Figure 8f). Liquid-ordered-like nature of cholesterol containing DOPC membranes has recently been found by NMR spectroscopy [68].

Discussion

The present study examined the partitioning behavior of fluorophores suitable for fluorescence microscopy imaging, between coexisting liquid-ordered and disordered phases. An important conclusion is that caution is necessary when choosing fluorescent membrane markers to label specific environments in either model membranes or biological membranes.

In particular, we found that a large variety of headgroup and chain-labeled fluorophores partition out of the L_o and into the L_d phase. The partitioning of DPPE and SPM-derived probes, as well as NBD-chol indicates that the phase preference of these fluorophores is dominated by the fluorescent label and not by the lipid backbone.

The partitioning of fluorophores depends on the lipid host system. The saturated-chain DiI derivatives partition increasingly into DSPC-containing L_o phases the longer the probe chain length. However, in the SPM system all DiI dyes were strongly excluded from the L_o phase. *This finding shows that sphingomyelin-based L_o phases have significantly different properties compared to phosphatidylcholine L_o phases.* A preferential interaction of cholesterol with sphingomyelin rather than phosphatidylcholine with long saturated chains has been suggested, but is discussed with great controversy [69,70]. We infer that the strong partitioning of DiI dyes in the SPM system out of L_o domains for all chain lengths indicates major headgroup packing constraints in the SPM system that are absent or reduced in the DSPC system. We note again that partitioning determined by fluorescence microscopy is qualitative in nature, due to reasons mentioned above. In fact, it was recently demonstrated that DiI dyes show higher molecular brightness in L_o phases compared to L_d and gel phases (Zhao and Feigenson et al, unpublished data). This fact, alone, however, cannot explain the chain length influence on optically determined dye partitioning, described above.

The saturated chain DiI probes show strong partitioning differences depending on their chain lengths in the DSPC system. The chain length influence of DiI partitioning between L_d phases and coexisting gel phases has been analyzed previously in DMPC [33], and in DPPC and DSPC [35]. In DMPC membranes, dialkyl DiI dyes with chain lengths of 10 to 14 carbons partitioned into the liquid phase, while dyes with 16 and 18 carbons partitioned into the gel phase. In DSPC membranes, the chain length influence of dialkyl DiI partitioning between gel and liquid phase is more pronounced, with a clear maximum partitioning into the gel that matched the probe hydrocarbon chain length [35]. This behavior is also observed in the DSPC-enriched L_o phase domains shown in Figure 4f–i and is probably due to approximate hydrophobic matching of dye and matrix lipid chains [33,35].

Polycyclic aromatic hydrocarbons were found in the present study to have preference for liquid-ordered phases with some dependence on the molecular structure of the dye. The relatively high photostability of naphthopyrene, perylene, rubicene and terrylene (compared to fluorescent cholesterol analogs) makes them suitable for studying the properties of L_o phases by fluorescence methods.

All of the L_o phase-preferring PAHs consist of a planar ring system. Although the molecular details that lead to the formation of liquid-ordered phases are not yet completely understood, it is known that the cholesterol/phospholipid interaction leads to an effective stretching of the acyl chains of the phospholipids by increasing the fraction of trans-configurations in the chain [71]. Furthermore, cholesterol preferentially associates with saturated chain sphingo- and phospholipids with high main phase transition temperature [72]. In particular, the flat α-surface of cholesterol associates with long chain saturated lipids such as sphingomyelin [73], whereas disorder-preferring lipids such as DOPC were observed by molecular dynamics simulations not to distinguish between the α-surface and the more rough β-surface of cholesterol. The partitioning behavior of polycyclic aromatic hydrocarbons discussed above indicates that hydrophobic, disk-shaped molecules can partition preferentially into the L_o phase.

Using fluorescence microscopy with polarized excitation light, we observed that PAHs tend to align their excitation dipole moment along the membrane normal in liquid-ordered phase membranes, but not in L_d phase membranes. A recent NMR study [74] examined the orientation of pyrene, a PAH similar in structure to the ones used in the present contribution, in lipid bilayer membranes. The normal to this disk-shaped molecule was found to align perpendicular to the membrane normal. The long axis of the molecule was found to align parallel to the membrane normal within a range of ±30°, in a disordered phase membrane of POPC [74]. This difference with our result that PAHs are not significantly oriented in L_d phase membranes might arise from the more ordered L_d phase in the partially dehydrated multilayer films of POPC [74]. On the other hand, the conclusion that PAHs orient with their longest axis along the membrane normal [74] is in agreement with our results for L_o phase membranes. For perylene, the angular intensity profile shows an interesting flattening of the peak intensity profile compared to naphthopyrene and terrylene. This phenomenon could indicate two distinct orientational populations of the fluorophore in the membrane [67], which has been suggested previously for perylene [59].

Our study of probe partitioning has been qualitative in nature. By comparing fluorescence intensities of fluorophores in coexisting fluid phases, it should in principle be possible to obtain quantitative results, i.e. partitioning coefficients of probes in *ternary* lipid mixtures, if phase coexistence is optically resolvable. Fluorescence microscopy imaging in that sense is advantageous over spectroscopic measurements of probe partitioning, which can yield quantitative measurements of partitioning coefficients in *binary*, but not in *ternary* mixtures, unless the phase diagram tie lines are known. The probe orientation measurements described and cited above, however, indicate that a quantitative microscopy measurement of fluorescence intensities to determine partitioning coefficients has to be carefully corrected for the effect of probe orientation within the membrane.

Conclusion

We have characterized a large variety of headgroup- and chain-labeled lipid analogs, cholesterol derivatives and PAHs for their partitioning between liquid-ordered and disordered phases. The following findings can be used as a guide for selecting fluorescence probes and lipid model systems in research aimed at elucidating membrane phase behavior with fluorescence methods.

1. Most lipid analogs partitioned strongly out of L_o and into L_d phases.
2. Polycyclic aromatic hydrocarbons partitioned out of L_d and into L_o phases, or showed equal phase partitioning.
3. Probe partitioning was found to depend on:

a. Characteristics of the fluorophore (i.e. the chain length and saturation/ unsaturation of fluorescent lipid analogs and the size and molecular structure of polycyclic intercalating fluorophores);

b. Nature of the host membrane lipids (DiI partitioning in the DSPC system was observed to be different from the SPM system).

Membrane fluorophore partitioning is expected to depend additionally on the mixing ratio of the host lipids, which is an effect that will be addressed in future experiments.

Acknowledgments

We acknowledge support from the National Science Foundation (Nanobiotechnology Center, an STC Program under Agreement No. ECS-9876771), the National Institutes of Health (AI18603), and from a National Institute of Biomedical Imaging and Bioengineering-National Institutes of Health Grant 9 P41 EB001976. GWF was supported by grants from the American Chemical Society PRF 38464-AC7 and the National Science Foundation MCB-0315330.

References

1. Simons K, Ikonen E. Functional Rafts in Cell Membranes. Nature 1997;387:569–572. [PubMed: 9177342]
2. Ikonen E. Roles of Lipid Rafts in Membrane Transport. Current Opinion in Cell Biology 2001;13:470–477. [PubMed: 11454454]
3. Parton RG, Richards AA. Lipid Rafts and Caveolae as Portals for Endocytosis: New Insights and Common Mechanisms. Traffic 2003;2003:724–738. [PubMed: 14617356]
4. Helms JB, Zurzolo C. Lipids as targeting signals: Lipid rafts and intracellular trafficking. Traffic 2004;5:247–254. [PubMed: 15030566]
5. Lommerse PHM, Spaink HP, Schmidt T. In vivo plasma membrane organization: results of biophysical approaches. Biochimica Et Biophysica Acta-Biomembranes 2004;1664:119–131.
6. Edidin M. The State of Lipid Rafts: From Model Membranes to Cells. Annual Review of Biophysics and Biomolecular Structure 2003;32:257–283.
7. Binder WH, Barragan V, Menger FM. Domains and rafts in lipid membranes. Angewandte Chemie-International Edition 2003;42:5802–5827.
8. Parton RG, Hancock JF. Lipid rafts and plasma membrane microorganization: insights from Ras. Trends in Cell Biology 2004;14:141–147. [PubMed: 15003623]
9. Zajchowski LD, Robbins SM. Lipid rafts and little caves - Compartmentalized signalling in membrane microdomains. European Journal of Biochemistry 2002;269:737–752. [PubMed: 11846775]
10. Brown DA, London E. Functions of Lipid Rafts in Biological Membranes. Ann Rev Cell Dev Biol 1998;14:111–136. [PubMed: 9891780]
11. Mayor S, Rao M. Rafts: Scale-dependent, active lipid organization at the cell surface. Traffic 2004;5:231–240. [PubMed: 15030564]
12. Munro S. Lipid Rafts: Elusive or Illusive? Cell 2003;115:377–388. [PubMed: 14622593]
13. McConnell HM, Vrljic M. Liquid-Liquid Immiscibility in Membranes. Ann Rev Biophys Biomol Struct 2003;32:469–492. [PubMed: 12574063]
14. Thomas JL, Holowka D, Baird B, Webb WW. Large-Scale Coaggregation of Fluorescent Lipid Probes With Cell-Surface Proteins. Journal of Cell Biology 1994;125:795–802. [PubMed: 8188747]
15. Hao MM, Mukherjee S, Maxfield FR. Cholesterol depletion induces large scale domain segregation in living cell membranes. Proceedings of the National Academy of Sciences of the United States of America 2001;98:13072–13077. [PubMed: 11698680]
16. Gidwani A, Holowka D, Baird B. Fluorescence Anisotropy Measurements of Lipid Order in Plasma Membranes and Lipid Rafts from RBL-2H3 Mast Cells. Biochemistry 2001;40:12422–12429. [PubMed: 11591163]
17. Gaus K, Gratton E, Kable EPW, Jones AS, Gelissen I, Kritharides L, Jessup W. Visualizing lipid structure and raft domains in living cells with two-photon microscopy. Proceedings of the National Academy of Sciences of the United States of America 2003;100:15554–15559. [PubMed: 14673117]

18. Varma R, Mayor S. GPI-anchored proteins are organized in submicron domains at the cell surface. Nature 1998;394:798–801. [PubMed: 9723621]
19. Kusumi A, Ike H, Nakada C, Murase K, Fujiwara T. Single-molecule tracking of membrane molecules: plasma membrane compartmentalization and dynamic assembly of raft-philic signaling molecules. Seminars in Immunology 2005;17:3–21. [PubMed: 15582485]
20. Vaz WLC, Melo E. Fluorescence spectroscopic studies on phase heterogeneity in lipid bilayer membranes. Journal of Fluorescence 2001;11:255–271.
21. Santos NC, Prieto M, Castanho MARB. Quantifying molecular partition into model systems of biomembranes: an emphasis on optical spectroscopic methods. Biochimica Et Biophysica Acta-Biomembranes 2003;1612:123–135.
22. Davenport L. Fluorescence Probes for Studying Membrane Heterogeneity. Methods in Enymology 1997;278:487–512.
23. Samsonov AV, Mihalyov I, Cohen FS. Characterization of Cholesterol-Sphingomyelin Domains and Their Dynamics in Bilayer Membranes. Biophysical Journal 2001;81:1486–1500. [PubMed: 11509362]
24. Dietrich C, Bagatolli LA, Volovyk ZN, Thompson NL, Levi M, Jacobson K, Gratton E. Lipid Rafts Reconstituted in Model Membranes. Biophysical Journal 2001;80:1417–1428. [PubMed: 11222302]
25. Veatch SL, Keller SL. Organization in Lipid Membranes Containing Cholesterol. Physical Review Letters 2002;89:268101-1–4. [PubMed: 12484857]
26. Veatch SL, Keller SL. Separation of Liquid Phases in Giant Vesicles of Ternary Mixtures of Phospholipids and Cholesterol. Biophysical Journal 2003;85:3074 – 3083. [PubMed: 14581208]
27. Kahya N, Scherfeld D, Bacia K, Poolman B, Schwille P. Probing lipid mobility of raft-exhibiting model membranes by fluorescence correlation spectroscopy. Journal of Biological Chemistry 2003;278:28109 – 28115. [PubMed: 12736276]
28. Baumgart T, Hess ST, Webb WW. Imaging coexisting fluid domains in biomembrane models coupling curvature and line tension. Nature 2003;425:821 – 824. [PubMed: 14574408]
29. Bagatolli LA, Gratton E. Two-photon fluorescence microscopy observation of shape changes at the phase transition in phospholipid giant unilamellar vesicles. Biophysical Journal 1999;77:2090–2101. [PubMed: 10512829]
30. Korlach J, Schwille P, Webb WW, Feigenson GW. Characterization of Lipid Bilayer Phases by Confocal Microscopy and Fluorescence Correlation Spectroscopy. Proceedings of the National Academy of Science USA 1999;96:8461 – 8466.
31. Feigenson GW, Buboltz JT. Ternary Phase Diagram of Dipalmitoyl-PC/Dilauroyl-PC/Cholesterol: Nanoscopic Domain Formation Driven by Cholesterol. Biophysical Journal 2001;80:2775 – 2788. [PubMed: 11371452]
32. Veatch SL, Keller SL. Miscibility phase diagrams of giant vesicles containing sphingomyelin. Physical Review Letters 2005;94
33. Klausner RD, Wolf DE. Selectivity of Fluorescenct Lipid Analogues for Lipid Domains. Biochemistry 1980;19:6199 – 6203. [PubMed: 7470460]
34. Huang, N-n; Florin-Casteel, K.; Feigenson, GW.; Spink, CH. Effects of Fluorophore Linkage Position of n-(9-anthroyloxy) fatty acids on probe distribution between coexisting gel and fluid phospholipid phases. Biochimica et Biophysica Acta 1988;939:124 – 130. [PubMed: 3349074]
35. Spink CH, Yeager MC, Feigenson GW. Partitioning Behavior of Indocarbocyanine Probes Between Coexisting Gel and Fluid Phase Model Membranes. Biochimica et Biophysica Acta 1990;1023:25 – 33. [PubMed: 2317494]
36. Beck A, Heissler D, Duportail G. Influence of the Length of the Spacer on the Partitioning Properties of Amphiphilic Fluorescent Membrane Probes. Chemistry and Physics of Lipids 1993;66:135 – 142. [PubMed: 8118914]
37. Loura LMS, Fedorov A, Prieto M. Partition of Membrane Probes in a Gel/Fluid Two-Component Lipid System: A Fluorescence Resonance Energy Transfer Study. Biochimica et Biophysica Acta 2000;1467:101 – 112. [PubMed: 10930513]
38. Mesquita RMRS, Melo E, Thompson TE, Vaz WLC. Partitioning of Amphiphiles between Coexisting Ordered and Disordered Phases in Two-Phase Lipid Bilayer Membranes. Biophysical Journal 2000;78:3019 – 3025. [PubMed: 10827980]

39. Pokorny A, Almeida PFF, Vaz WLC. Association of a Fluorescent Amphiphile with Lipid Bilayer Vesicles in Regions of Solid-Liquid-Disordered Phase Coexistence. Biophysical Journal 2001;80:1384 – 1394. [PubMed: 11222299]
40. Wang TY, Silvius JR. Different Sphingolipids Show Differential Partitioning into Sphingolipid/Cholesterol-Rich Domains in Lipid Bilayers. Biophysical Journal 2000;79:1478 – 1489. [PubMed: 10969009]
41. Wang TY, Leventis R, Silvius JR. Fluorescence evaluation of molecular partitioning into lipid 'rafts' (liquid-ordered domains) in lipid model membranes. Molecular Biology of the Cell 2000;11:4a–5a.
42. Wang TY, Leventis R, Silvius JR. Partitioning of lipidated peptide sequences into liquid-ordered lipid domains in model and biological membranes. Biochemistry 2001;40:13031–13040. [PubMed: 11669641]
43. Wang TY, Silvius JR. Sphingolipid-Partitioning into ordered domains in Cholesterol-free and cholesterol containing lipid bilayers. Biophysical Journal 2003;84:367 – 378. [PubMed: 12524290]
44. Koivusalo M, Alvesalo J, Virtanen JA, Somerharju P. Partitioning of pyrene-labeled phospho- and sphingolipids between ordered and disordered bilayer domains. Biophysical Journal 2004;86:923–935. [PubMed: 14747328]
45. Gruber HJ, Schindler H. External Surface and Lamellarity of Lipid Vesicles - a Practice-Oriented Set of Assay-Methods. Biochimica Et Biophysica Acta-Biomembranes 1994;1189:212–224.
46. Fischer RT, Stephenson FA, Shafiee A, Schroeder F. Delta-5,7,9(11)-Cholestatrien-3beta-Ol - a Fluorescent Cholesterol Analog. Chemistry and Physics of Lipids 1984;36:1–14. [PubMed: 6518610]
47. Akashi K, Miyata H, Itoh H, Kinosita K. Preparation of Giant Liposomes in Physiological Conditions and Their Characterization under an Optical Microscope. Biophysical Journal 1996;71:3242 – 3250. [PubMed: 8968594]
48. Mathivet L, Cribier S, Devaux PF. Shape Change and Physical Properties of Giant Phospholipid Vesicles Prepared in the Presence of an AC Electric Field. Biophysical Journal 1996;70:1112–1121. [PubMed: 8785271]
49. Ayuyan AG, Cohen FS. Lipid peroxides promote large rafts: effects of excitation of probes in fluorescence microscopy and electrochemical reactions during vesicle formation. Biophysical Journal Biofast. 200610.1529/biophysj.106.087387
50. Maier O, Oberle V, Hoekstra D. Fluorescent lipid probes: some properties and applications (a review). Chemistry and Physics of Lipids 2002;116:3–18. [PubMed: 12093532]
51. Gagescu R, Demaurex N, Parton RG, Hunziker W, Huber LA, Gruenberg J. The recycling endosome of Madin-Darby canine kidney cells is a mildly acidic compartment rich in raft components. Molecular Biology of the Cell 2000;11:2775–2791. [PubMed: 10930469]
52. Puri V, Watanabe R, Singh RD, Dominguez M, Brown JC, Wheatley CL, Marks DL, Pagano RE. Clathrin-dependent and -independent internalization of plasma membrane sphingolipids initiates two Golgi targeting pathways. Journal of Cell Biology 2001;154:535–547. [PubMed: 11481344]
53. Schroeder RJ, Ahmed SN, Zhu YZ, London E, Brown DA. Cholesterol and sphingolipid enhance the Triton X-100 insolubility of glycosylphosphatidylinositol-anchored proteins by promoting the formation of detergent-insoluble ordered membrane domains. Journal of Biological Chemistry 1998;273:1150–1157. [PubMed: 9422781]
54. Scherfeld D, Kahya N, Schwille P. Lipid dynamics and domain formation in model membranes composed of ternary mixtures of unsaturated and saturated phosphatidylcholines and cholesterol. Biophysical Journal 2003;85:3758–3768. [PubMed: 14645066]
55. Veatch SL, Polozov IV, Gawrisch K, SL K. Liquid domains in vesicles investigated by NMR and fluorescence microscopy. Biophysical Journal 2004;86:2910–2922. [PubMed: 15111407]
56. Scheidt HA, Mueller P, Herrmann A, Huster D. The potential of fluorescent and spin-labeled steroid analogs to mimic natural cholesterol. The Journal of Biological Chemistry 2003;278:45563–45569. [PubMed: 12947110]
57. Lakowicz JR, Knutson JR. Hindered Depolarizing Rotations of Perylene in Lipid Bilayers - Detection by Lifetime-Resolved Fluorescence Anisotropy Measurements. Biochemistry 1980;19:905–911. [PubMed: 7356968]

58. Chong PLG, van der Meer BW, Thompson TE. The Effects of Pressure and Cholesterol on Rotational Motions of Perylene in Lipid Bilayers. Biochimica et Biophysica Acta 1984;813:253–265. [PubMed: 3970923]
59. Zandvoort MAMJ, Gerritsen HC, van Ginkel G, Levine YK, Tarroni R, Zannoni C. Distribution of Hydrophobic Probe Molecules in Lipid Bilayers. 2. Time-Resolved Fluorescence Anisotropy Study of Perylene in Vesicles. Journal of Physical Chemistry B 1997;101:4149–4154.
60. Rademacher A, Maerkle S, Langhals H. Loesliche Perylen-Fluoreszenzfarbstoffe mit hoher Photostabilitaet. Chem Ber 1982;115:2927–2934.
61. Knutson JR, Davenport L, Brand L. Anisotropy Decay Associated Fluorescence-Spectra and Analysis of Rotational Heterogeneity.1. Theory and Applications. Biochemistry 1986;25:1805–1810. [PubMed: 3707911]
62. Lentz BR. Use of Fluorescent-Probes to Monitor Molecular Order and Motions within Liposome Bilayers. Chemistry and Physics of Lipids 1993;64:99–116. [PubMed: 8242843]
63. Lentz BR, Barrow DA, Hoechli M. Cholesterol-Phosphatidylcholine Interactions in Multilamellar Vesicles. Biochemistry 1980;19:1943–1954. [PubMed: 6892884]
64. Axelrod D. Carbocyanine Dye Orientation in Red-Cell Membrane Studied by Microscopic Fluorescence Polarization. Biophysical Journal 1979;26:557–573. [PubMed: 263688]
65. Florinecasteel K. Phospholipid Order in Gel-Phase and Fluid-Phase Cell-Size Liposomes Measured by Digitized Video Fluorescence Polarization Microscopy. Biophysical Journal 1990;57:1199–1215. [PubMed: 2393705]
66. Bagatolli LA, Gratton E. Two Photon Fluorescence Microscopy of Coexisting Lipid Domains in Giant Unilamellar Vesicles of Binary Phospholipid Mixtures. Biophysical Journal 2000;78:290–305. [PubMed: 10620293]
67. Florinecasteel, K. Video imaging of lipid order. Elsevier; 1999.
68. Warschawski DE, Devaux PF. Order parameters of unsaturated phospholipids in membranes and the effect of cholesterol: a H-1-C-13 solid-state NMR study at natural abundance. European Biophysics Journal with Biophysics Letters 2005;34:987–996. [PubMed: 15952018]
69. Guo W, Kurze V, Huber T, Afdhal NH, Beyer K, Hamilton JA. A Solid-State NMR Study of Phospholipid-Cholesterol Interactions: Sphingomyelin-Cholesterol Binary Systems. Biophysical Journal 2002;83:1465–1478. [PubMed: 12202372]
70. Ohvo-Rekila H, Ramstedt B, Leppimaki P, Slotte JP. Cholesterol interactions with phospholipids in membranes. Progress in Lipid Research 2002;41:66–97. [PubMed: 11694269]
71. Sankaram MB, Thompson TE. Modulation of Phospholipid Acyl Chain Order by Cholesterol. A Solid-State 2H Nuclear Magnetic Resonance Study. Biochemistry 1990;29:10676–10684. [PubMed: 2271675]
72. Silvius JR. Role of cholsterol in lipid raft formation: lessons from lipid model systems. Biochimica et Biophysica Acta 2003;1610:174–183. [PubMed: 12648772]
73. Pandit SA, Jakobsson E, Scott HL. Simulation of the early stages of nano-domain formation in mixed bilayers of sphingomyelin, cholesterol, and dioleylphosphatidylcholine. Biophysical Journal 2004;87:3312–3322. [PubMed: 15339797]
74. Hoff B, Strandberg E, Ulrich AS, Tieleman DP, Posten C. H-2-NMR study and molecular dynamics simulation of the location, alignment, and mobility of pyrene in POPC bilayers. Biophysical Journal 2005;88:1818–1827. [PubMed: 15596514]

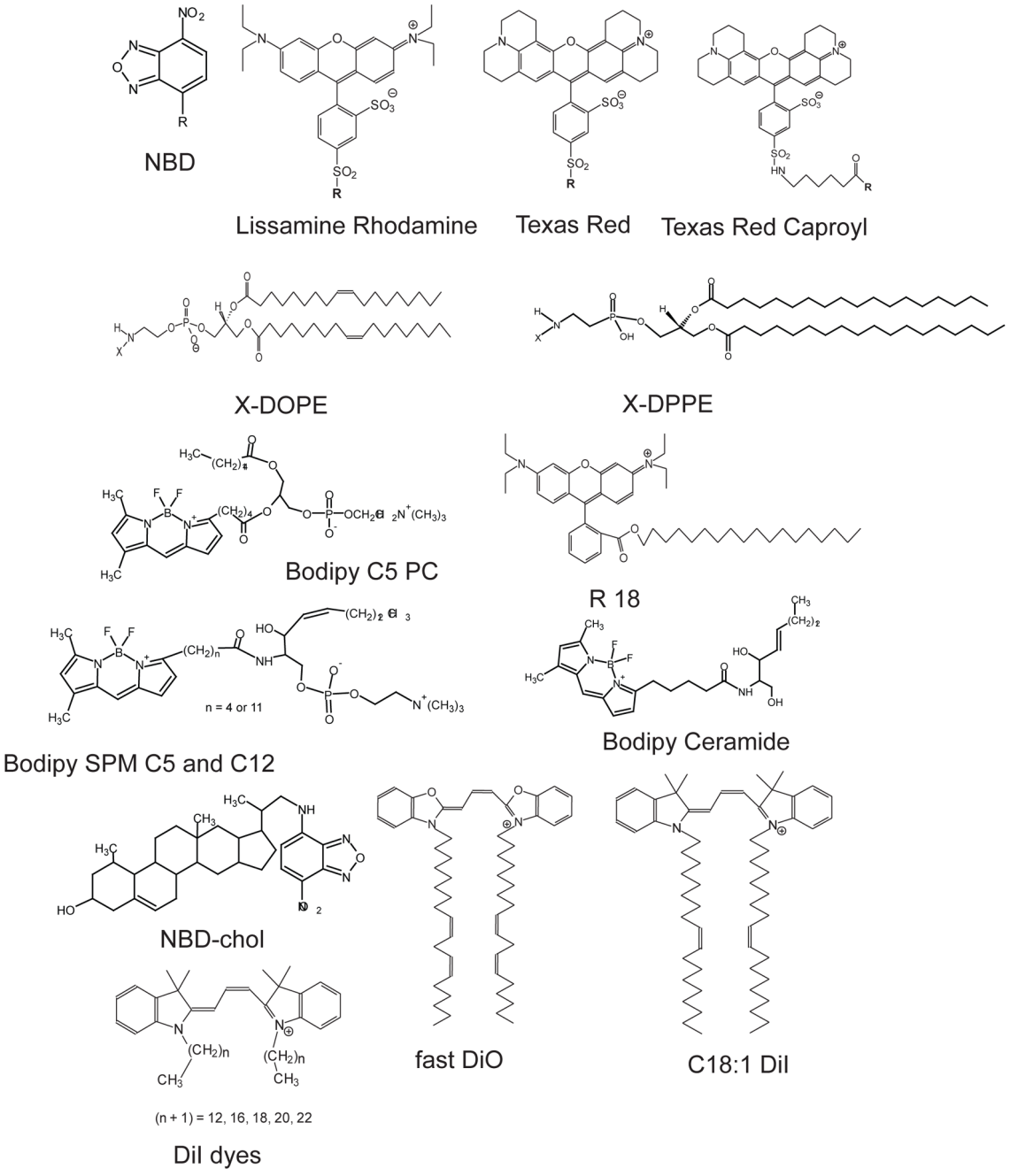

Figure 1.

Lipid analog dyes used for partitioning studies: mostly disordered phase preferring probes (see the text for the exception of long chain DiI probes in the DSPC system).

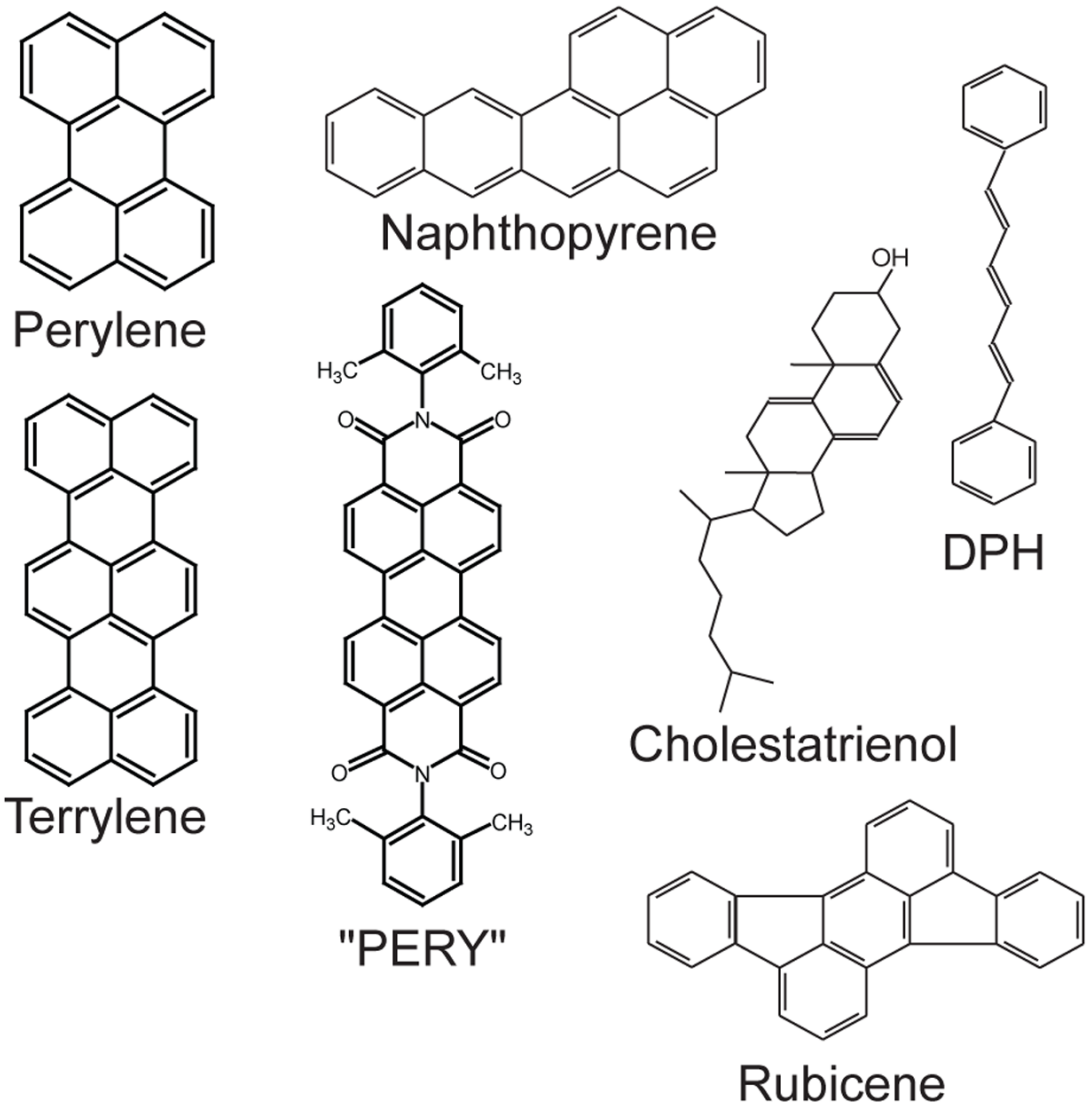

Figure 2.

PAH dyes and DPH used for partitioning and probe orientation studies. The molecules perylene, naphthopyrene, terrylene, cholestatrienol and rubicene partition equally or preferentially into the L_o phase. The dye PERY is L_d phase preferring and DPH does not show preferential partitioning.

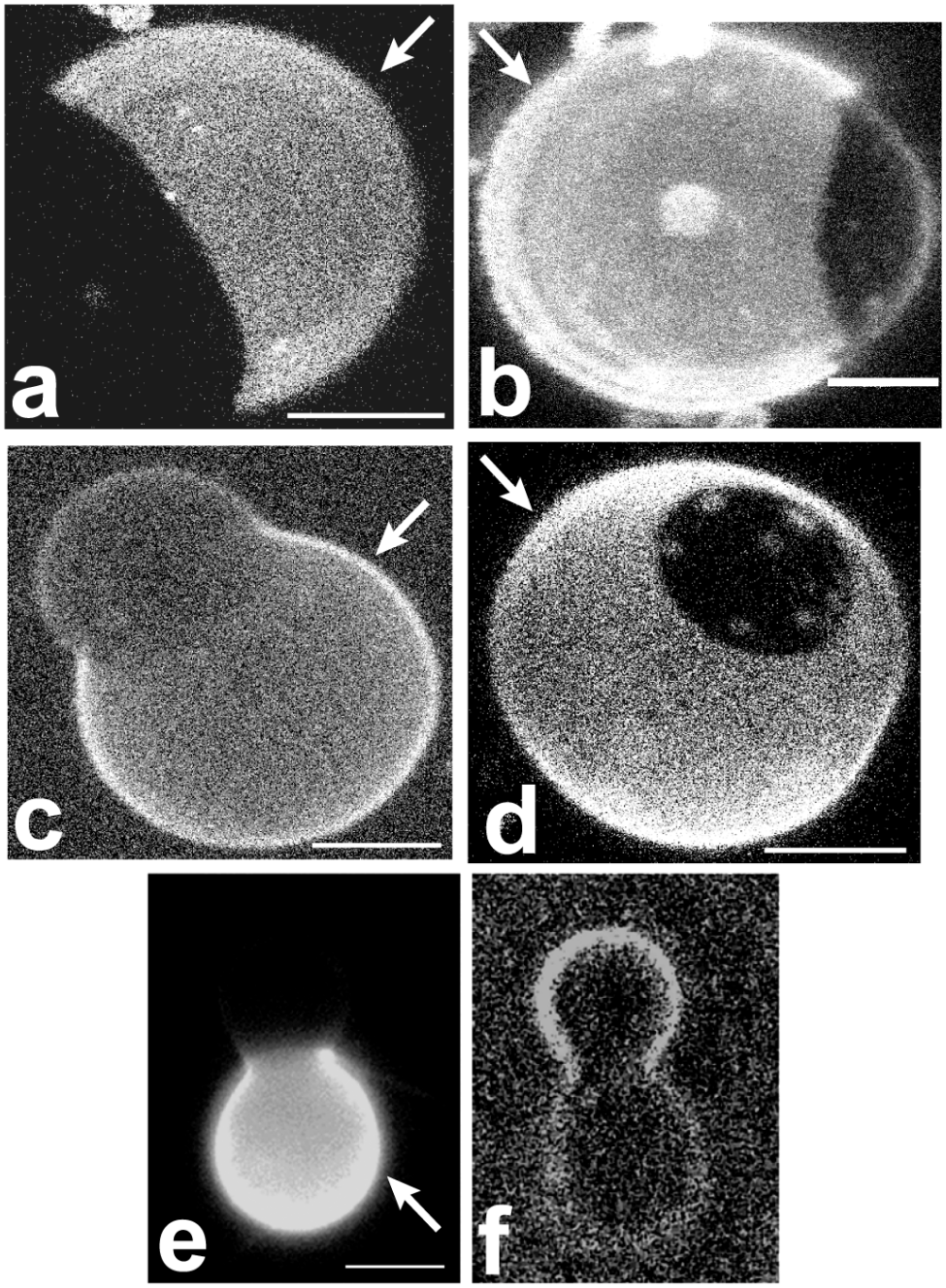

Figure 3.

Hemispherical projections of confocal images of GUVs, labeled with a variety of different membrane dyes. In all panels of this figure, and all following figures, the L_d phase is indicated with a white arrow. Panels a–d refer to composition 27/50/23 (DSPC/DOPC/chol), where the L_d phase is the majority phase. a) Liss-Rho-DOPE: L_d phase partitioning preference is found for this dye as well as other dyes with unsaturated chains. b) Bodipy-PC: Lipids labeled in the chain region partition into the L_d phase. c) and d): NBD-DPPE and Liss-Rho-DPPE, respectively: long and saturated chain headgroup labeled lipids prefer the L_d phase. e) and f): Rho-DOPE (e) and cholestatrienol (f) labeling of a vesicle in the SPM system with composition

30/45/25 (SPM/DOPC/chol). Cholestatrienol is observed to preferentially partition into the L_o phase, whereas Rho-DOPE labels the Ld phase. Bars: 5 μm (a–d) and 15 μm (e–f).

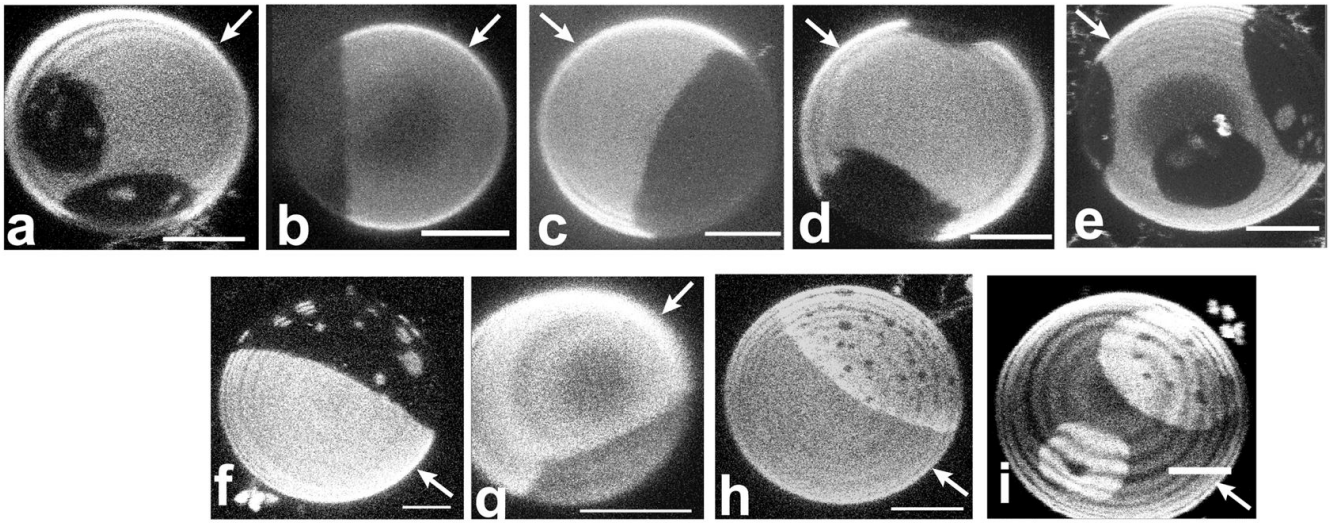

Figure 4.

Confocal images of GUVs in the SPM/DOPC/chol system (a–e) and the DSPC/DOPC/chol system (f–i). In all images the L_d phase is the majority phase (i.e. the phase with larger area fraction). The following DiI fluorophores were used for labeling: (a & f), DiI-C12:0; (b & g), DiI-C16:0; (c & h), DiI-C18:0; (d) DiI C20:0; and (e & i), DiI C22:0. In the SPM system, DiI dyes of all chain lengths partitioned into the L_d phase as in Fig 4a–4e. In the DSPC system, however, long saturated chain DiIs partitioned preferentially into the L_o phase as in Fig 4h–4i. Note that the concentric shading in several images is due to z scan inhomogeneity, not membrane inhomogeneity. Bar: 5 μm.

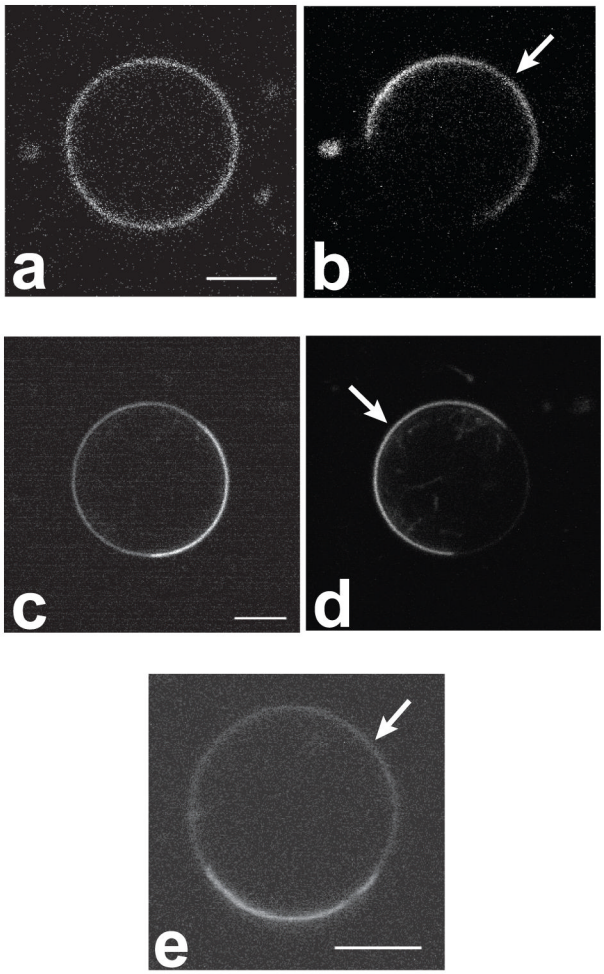

Figure 5.

Equatorial images of GUVs obtained by two-photon laser scanning microscopy at an excitation wavelength of λ = 750 nm, indicating the partitioning of polycyclic fluorescent hydrocarbons. Images report on SPM system. a) perylene fluorescence not distinguishing L_o and L_d phase; b) same vesicle as in a) the red fluorophore Liss-Rho-DOPE is used to image the L_d phase c) naphthopyrene fluorescence showing phase separation; d) same vesicle as in c), Liss-Rho-DOPE fluorescence; and e) terrylene fluorescence showing phase separation. Polycyclic aromatic hydrocarbons show equal partitioning to significant partitioning into the L_o phase, with a degree of partitioning that depends on the molecular structure of the PAH. Bar: 5 μm.

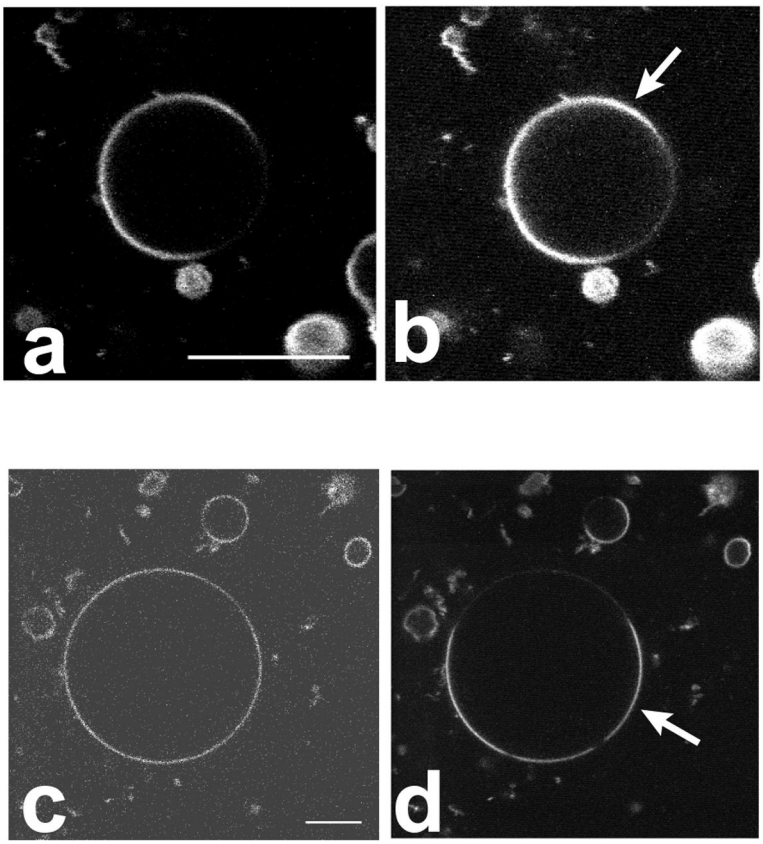

Figure 6.
Equatorial images of GUVs in the SPM system obtained by two-photon laser scanning microscopy at an excitation wavelength of $\lambda = 750$ nm, showing the partitioning of the fluorescent membrane dyes N,N, bis-dimethylphenyl 2,4,6,8, perylenetetracarbonyl diamide ("PERY") (a) and DPH (c). For comparison, the partitioning of Liss-Rho-DOPE is shown in the right image of each row (c and d), for the same vesicle imaged on the left-hand side. "PERY" strongly partitions out of L_o phases and DPH shows negligible phase preference. Bar: 12 μm.

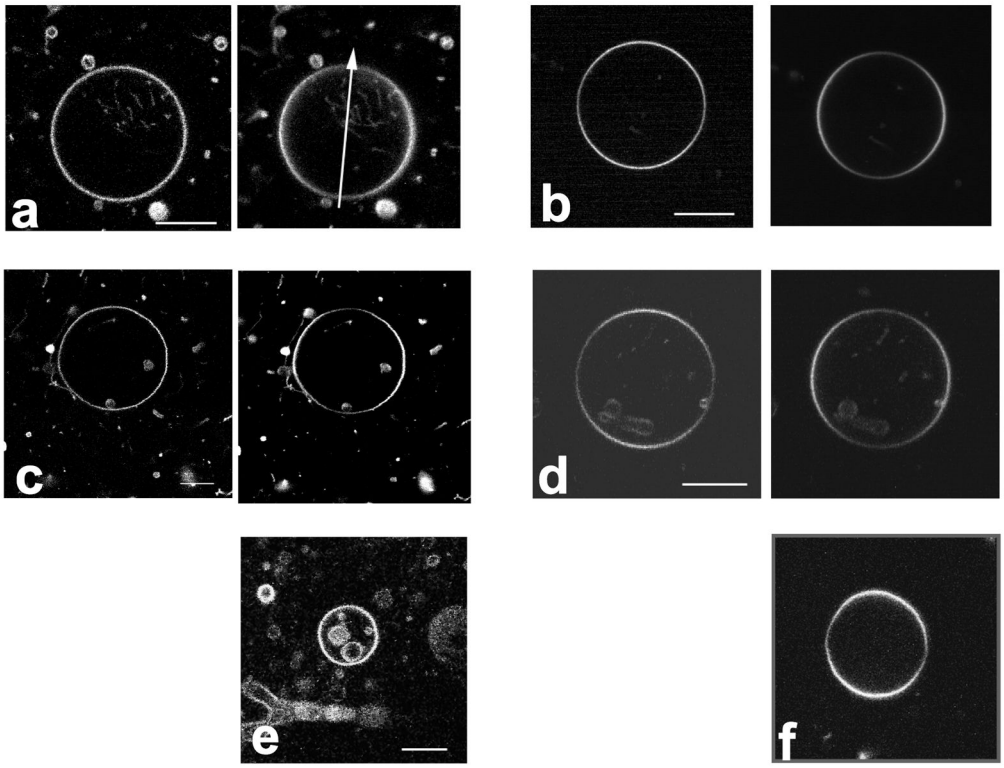

Figure 7.

Equatorial images of GUVs obtained by two-photon laser scanning microscopy at an excitation wavelength of $\lambda = 750$ nm. Vesicles were illuminated with linear polarization along the arrow in a). The observed angular intensity patterns demonstrate the orientation (see text for details) of polycyclic aromatic hydrocarbons in L_d phase vesicles (DOPC) and L_o phase vesicles (SPM/chol = 1:1). a) perylene L_d; b) perylene L_o; c) naphthopyrene L_d; d) naphthopyrene L_o; e) terrylene L_d; and f) terrylene L_o. In case of images a) – d), the right image in each panel shows the angular fluorescence pattern of Liss-Rho-DOPE in the same vesicle, for comparison. Whereas PAH fluorescence intensities are constant around the vesicle perimeter in case of L_d phase membranes, L_o phase membranes PAHs show an angular intensity pattern that is rotated by 90° compared to the intensity pattern of Liss-Rho-DOPE fluorescence. This finding indicates that PAHs tend to orient with their long axes parallel to the membrane normal in L_o phase membranes, but not in L_d phase membranes. Bar: 12 μm.

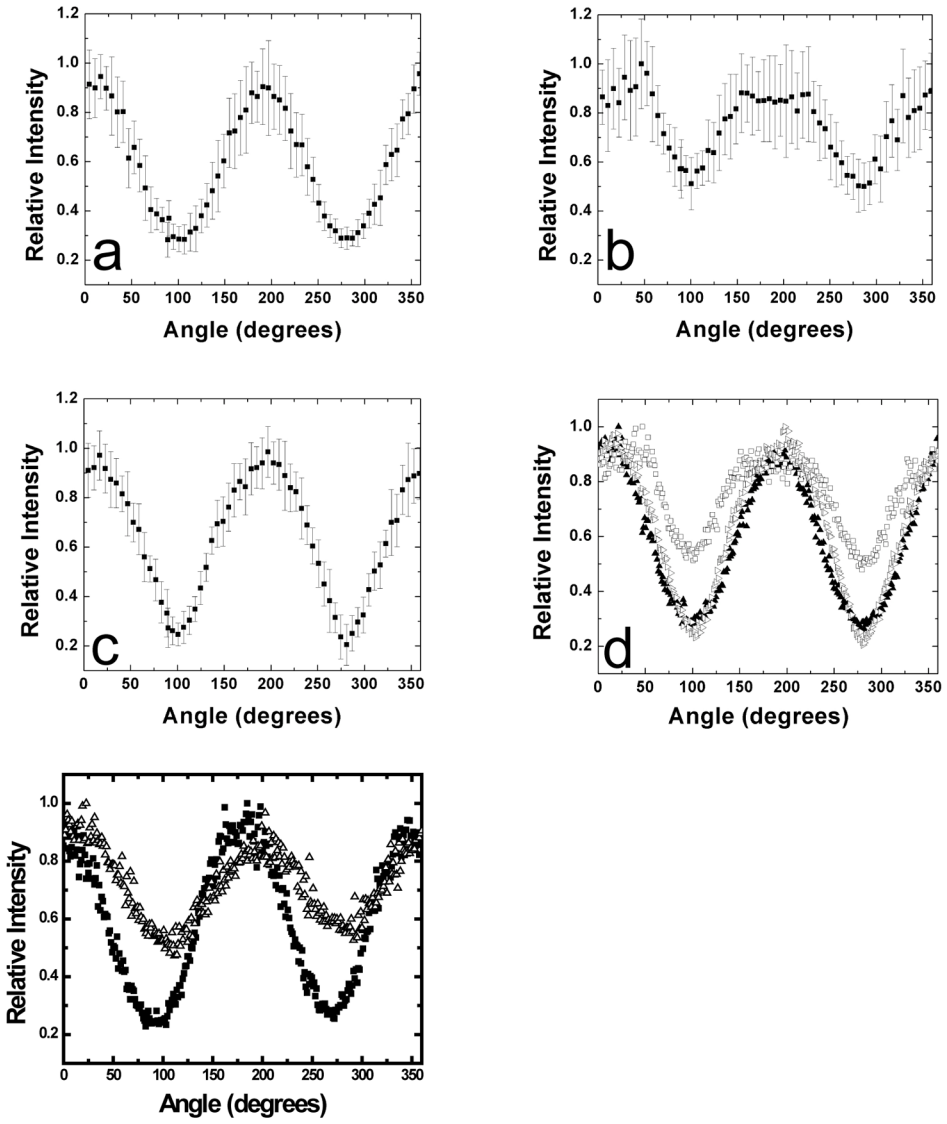

Figure 8.

Angular intensity distributions of polycyclic aromatic hydrocarbons (PAHs) in L_o phase vesicles and DOPC vesicles containing cholesterol. Intensity distributions were obtained from fluorescence images equivalent to those shown in Figure 7, of vesicles illuminated with linearly polarized excitation light. The error bars refer to standard deviations that correspond to ten individual measurements. a) naphthopyrene, b) perylene, c) terrylene, d) a combination of the three plots for comparison. In the case of perylene, a shallower intensity profile is obtained compared to naphthopyrene and terrylene, indicating less confined orientations of perylene in L_o phase membranes. This finding parallels the partition behavior of perylene compared to naphthopyrene and terrylene. The characteristic flattening of perylene fluorescence near the maximum intensities (see panel b) could indicate two different orientational populations of this fluorophore [64]. e) Naphthopyrene angular intensity distributions in DOPC/chol = 7:3 vesicles. Increased cholesterol content leads to orientational confinement of the fluorescence probe, albeit to a weaker extent compared to SPM (see the comparison in panel f of the DOPC/chol = 7:3 (open triangles), and SPM/chol=7:3 measurements (filled circles)). Equivalent behavior is found for perylene and terrylene (data not shown).

Table 1

Partitioning of fluorescent lipid mimetic molecules between two coexisting fluid membrane phases in the ternary lipid mixture SPM/DOPC/cholesterol.

Fluorescent probe	Partitioning preference (0 indicates no preference)
X-DOPE	L_d
DiI C18:1	L_d
Fast DiO	L_d
Bodipy PC	L_d
SPM C_n Bodipy	L_d
Bodipy Ceramide	L_d
X-DPPE	L_d
Y-DPPE	L_d
R18	L_d
NBD-chol	L_d
Cholestatrienol	L_o
DiI C_m:0	L_d
Naphthopyrene	L_o
Perylene	=
Rubicene	=
Terrylene	L_o
DPH	=
“PERY”	L_d

The partitioning behavior of the fluorophores indicated in this table for the SPM system is qualitatively similar in the DSPC system. The saturated chain DiI dyes are the important exception (see Table 2). X = NBD, Lissamine rhodamine. Y = Texas red, N-caproyl-Texas red. n = 5, 12. m = 12, 16, 18, 20, 22.

Table 2

Comparison of the partitioning of saturated chain dialkylindocarbocyanine dyes of varying chain lengths in ternary lipid mixtures with liquid phase coexistence.

Fluorescent probe	Phase preference SPM system	Phase preference DSPC system
DiI C12:0	L_d	L_d
DiI C16:0	L_d	L_d
DiI C18:0	L_d	L_o
DiI C20:0	L_d	L_o
DiI C22:0	L_d	L_o